Annals of Nuclear Medicine (2022) 36:610–622
https://doi.org/10.1007/s12149-022-01742-8

ORIGINAL ARTICLE

^{68}Ga-DOTA-FAPI-04 PET/CT imaging in radioiodine-refractory differentiated thyroid cancer (RR-DTC) patients

Yun Chen[1] · Shan Zheng[1] · Jiaying Zhang[1] · Shaobo Yao[1,2] · Weibing Miao[1,2]

Received: 23 September 2021 / Accepted: 10 April 2022 / Published online: 12 May 2022

Abstract

Objective This study aimed to assess the potential of ^{68}Ga-DOTA-FAPI-04 PET/CT for the detection of the radioiodine-refractory differentiated thyroid cancer (RR-DTC) lesions.

Methods We analyzed the ^{68}Ga-DOTA-FAPI-04 PET/CT imaging data of 24 RR-DTC patients (7 men and 17 women; 49.6 ± 10.5 year). Clinical data were collected including history, last post-therapeutic radioiodine whole body scan, contemporary CT, thyroglobulin, and antithyroglobulin. Target lesions were selected and measured by the RECIST 1.1. The mean growth rates of the target lesions in the past 6 months were recorded. Tumor uptake of lesions were quantified by SUVmax and the tumor-to-background ratios. The correlation between SUVmax and target lesion growth rate and thyroglobulin was analyzed.

Results On patient-based analysis, positive metastases were detected in 87.5% (21/24) patients. Except for the lymph node (LN) metastasis of 3 patients (patient 6, 12 and 17#) and the lung metastasis of another 3 patients (patient 9, 13 and 21#), most of the lesions were positive on ^{68}Ga-DOTA-FAPI-04 PET/CT images, including LN metastasis and distant metastasis such as lung, bone and pleura. There were altogether 33 target lesions including 30 lung metastases and 3 LN metastases with the mean SUVmax and the growth rate were 4.25 and 6.51%, respectively. SUVmax was statistically associated with the growth rates of the target lesions ($p = 0.047$). No statistically significant correlation was found between the SUVmax and the serum thyroglobulin levels ($p = 0.139$).

Conclusions ^{68}Ga-DOTA-FAPI-04 PET/CT has a promising detection rate for RR-DTC metastasis. The FAPI uptake of the tumor may provide a potential therapeutic target for RR-DTC.

Trial registry NIH Clinical Trials.gov (NCT04499365).

Keywords ^{68}Ga-DOTA-FAPI-04 · PET/CT · Radioiodine-refractory DTC · Metastasis

Introduction

Thyroid cancer is the most common endocrine malignancy with a growing incidence, ranking ninth in the global incidence of cancer [1]. The majority of thyroid cancers are differentiated thyroid cancer (DTC). Optimistic prognosis of DTC is commonly achieved because of its adequate management strategies, such as surgery, radioiodine (^{131}I) treatment, and levothyroxine therapy. However, radioiodine-refractory DTC (RR-DTC) have become the main cause of disease-specific death with a 10-year survival rate as low as 10% [2], which represents a very difficult management situation.

Cancer guidelines of the American Thyroid Association recommend the use of ^{18}F-FDG PET/CT for the detection of RR-DTC lesions [3]. However, ^{18}F-FDG is neither a tumor

Yun Chen and Shan Zheng shared first authorship.

✉ Shaobo Yao
yaoshaobo008@163.com

✉ Weibing Miao
miaoweibing@126.com

Yun Chen
chenyun200103305@126.com

Shan Zheng
zhengshan1982@126.com

[1] Department of Nuclear Medicine, The First Affiliated Hospital of Fujian Medical University, No. 20 Chazhong Road, Taijiang District, Fuzhou 350005, Fujian Province, China

[2] Fujian Provincial Key Laboratory of Precision Medicine for Cancer, The First Affiliated Hospital of Fujian Medical University, Fuzhou 350005, Fujian Province, China

specific tracer nor a therapeutic one. Novel tracers with a specific target are urgently needed for diagnosis and therapy.

^{68}Ga-DOTA-FAPI-04 is a novel radiotracer targeting fibroblast activation protein (FAP), which is highly expressed in cancer-associated fibroblasts (CAFs) of many epithelial carcinomas [4–6]. ^{68}Ga-DOTA-FAPI-04 serves as an alternative to ^{18}F-FDG for the assessment of malignant tumors and adds important diagnostic value in the context of challenging ^{18}F-FDG PET/CT cancer subtypes in previous studies [7, 8]. The uptake of ^{68}Ga-DOTA-FAPI-04 was observed in many various tumor entities like thyroid cancer [4, 9–13]. Unlike ^{18}F-FDG, radiolabeled FAP inhibitors (FAPI) makes FAP-imaging and therapy possible. This study first reported ^{68}Ga-DOTA-FAPI-04 PET/CT imaging in a cohort of RR-DTC patients.

Materials and methods

Patients

This study was approved by the Clinical Research Ethics Committee of the First Affiliated Hospital of Fujian Medical University and conducted in accordance with the 1964 Declaration of Helsinki and its later amendments or comparable ethical standards (ID 2019-XJS-1130). This study was also registered online at NIH ClinicalTrials.gov (NCT04499365). Informed written consent was obtained from all of these enrolled patients.

RR-DTC is classified in patients with appropriate TSH stimulation and iodine preparation in four basic ways according to 2015 American Thyroid Association Management Guidelines [3]. From December 2020 to November 2021, 24 RR-DTC patients were recruited from the First Affiliated Hospital of Fujian Medical University. The eligibility criteria were as follows: (i) adult patients (aged 18 years or older); (ii) a negative pregnancy test; (iii) clinically acceptable renal and hepatic function; (iv) RR-DTC patients with structural lesions, treated by ^{131}I more than twice.

Radiopharmaceutical preparation

Good-manufacturing-practice (GMP) grade precursors DOTA-FAPI-04 were purchased from Jiangsu Huayi Technology Co. (Jiangsu, China). $^{68}GaCl_3$ was eluted from a [^{68}Ge]/[^{68}Ga] generator (JSC Isotope, Obninsk, Russia) using 5 mL of 0.1 M hydrochloride acid. Radiolabeling was performed manually in a hot cell as previously reported [14, 15]. Radiochemical purity of the final product was over 95%. The median specific activity was 1.67 (range 1.25–2.76) MBq/ug.

PET/CT imaging

The injection activity of ^{68}Ga-DOTA-FAPI-04 was calculated according to the patient's weight (1.85–2.22 MBq/kg). Before imaging, all the subjects were asked to urinate completely. The emission scan using a hybrid PET/CT scanner (Biograph mCT 64, SIEMENS, Germany) began 30 min after intravenous injection. The patient was supine on the examination bed. CT scan was performed from the head to upper thighs. The following parameters for the CT scan were used: tube voltage of 110 kV, current of 120 mA, and slice thickness of 3 mm, reconstruction interval 1 mm with a sharp reconstruction kernelD. A PET scan was immediately performed after the CT scan in 3D acquisition mode with 6–8 bed positions and 3 min/position. TOF mode/reconstruction is utilized. All the obtained data were transferred to the MultiModality Workstation (syngoTM MI, SIEMENS, Germany); data were reconstructed using the ordered subset expectation maximization algorithm (two iterations and 21 subsets); CT data were used for attenuation correction; and the reconstructed images were then co-registered and displayed. An additional chest CT was performed with the patient in the supine position at full inspiration, without intravenous contrast medium. The CT acquisition protocol of chest CT 6 months ago was similar to that of FAPI PET/CT imaging.

Image analysis

Studies were analyzed by a group of two experienced nuclear medicine physicians (W Miao and S Chen). Any difference in opinion was resolved by consensus. All metastases were confirmed by pathological examination, medical imaging including post-therapeutic radioiodine whole body scan, ^{131}I single photon emission computed tomography/computed tomography (SPECT/CT), high-resolution ultrasonography (US) and CT, serum thyroglobulin (TG) test, and clinical follow-up of at least 6 months as well (Table 1). In addition to elevated TG level, a diagnosis of metastatic lymph node (LN) was established in terms of at least two of the following signs: microcalcification, cystic aspect, peripheral vascularization, and hyperechogenicity in US examination [16, 17]. Because of ethical concerns, biopsies and histopathology were not available for most of the analyzed metastases except for lung metastasis in six patients, pleura metastasis in one patient and bone metastasis in three patients (Table 1).

RR-DTC metastases were coded as positive if the activity exceeded that of the adjacent background tissues. The positive lesions found on FAPI imaging were divided into target lesions and non-target lesions according to the

Table 1 Clinical characteristics ($n=24$)

Patient no.	Gender	Age	Pathologic type	No of RAI	Accumulated dose (mCi)	Metastatic lesions		Last Rx-WBS	Confirmation of metastatic lesions	TG (ng/mL)	TGAb (IU/mL)	$BRAFV^{600E}$ mutation
						Site	Size (cm)					
1	Female	33	PTC	3	400	Lung	1.6	Negative	CT imaging and follow-up	2056	11.4	NA
2	Female	66	PTC	4	580	Left thyroid bed	3.4	Positive	Rx-WBS	57.8	< 10	NA
						LN, cervical + mediastinal	1.2	Negative	US/CT imaging and follow-up			
						Lung	2.8	Negative	CT imaging and follow-up			
						Bone, C7	–	Negative	CT imaging and follow-up			
3	Female	62	PTC (follicular subtype)	2	310	LN, cervical + mediastinal	1.1	Negative	US/CT imaging and follow-up	519	< 10	NA
						Lung	2.1	Negative	CT imaging and follow-up			
4	Female	54	PTC	2	400	Lung	1.1	Negative	Pathology	3.74	< 10	NA
5	Female	59	PTC	2	350	LN, cervical + mediastinal	1.1	Negative	US/CT imaging and follow-up	96.7	< 10	+
						Lung	2.3	Negative	Pathology			
6	Female	42	PTC	8	1105	LN, cervical + supraclavicular + mediastinal	0.9	Positive	Rx-WBS	1611	10	NA
						Lung	2.0	Positive	Rx-WBS and CT imaging			
						Left pleura	2.3	Negative	Pathology			
7	Female	56	PTC	3	450	Lung	0.8	Negative	CT imaging and follow-up	13.1	< 10	-
8	Male	52	PTC	4	750	LN, cervical + mediastinal	2.4	Negative	US/CT imaging and follow-up	> 5000	55.1	NA
						Lung	0.7	Negative	CT imaging and follow-up			
						Bone, skull + sternum + vertebral body, etc	–	Negative	Pathology			
9	Female	65	PTC	5	950	LN, cervical + mediastinal	1.0	Positive	Rx-WBS	0.25	2854	NA
						Lung	0.4	Negative	Rx-WBS			
10	Male	58	PTC	5	850	Lung	1.3	Positive	Rx-WBS and CT imaging	615	13.7	NA

Table 1 (continued)

Patient no.	Gender	Age	Pathologic type	No of RAI	Accumulated dose (mCi)	Metastatic lesions		Last Rx-WBS	Confirmation of metastatic lesions	TG (ng/mL)	TGAb (IU/mL)	$BRAFV^{600E}$ mutation
						Site	Size (cm)					
11	Female	25	PTC	3	410	LN, cervical + mediastinal	1.2	Negative	US/CT imaging and follow-up	612	12.0	NA
						Lung	1.0	Negative	CT imaging and follow-up			
12	Female	43	PTC	8	1480	Lung	0.6	Positive	Rx-WBS	51.9	10.1	NA
						LN, cervical + supraclavicular	0.6	Negative	US/CT imaging and follow-up			
13	Male	39	PTC	9	1720	Bone, ilium + acetabulum	–	Positive	Pathology	138	17.7	NA
						Lung	0.2	Positive	Rx-WBS			
14	Male	56	FTC	8	1480	Bone, sternum + L4	–	Positive	Pathology	1269	21.5	NA
15	Female	54	PTC/FTC	3	550	Lung	3.3	Negative	Pathology	1446	19.0	NA
16	Male	47	PTC	2	240	Lung	1.8	Negative	Pathology	1702	< 15	NA
						LN, mediastinal	2.0	Negative	US/CT imaging and follow-up			
						Right pleura	1.2	Negative	US/CT imaging and follow-up			
						Bone, left ilium	–	Negative	US/CT imaging and follow-up			
17	Male	45	PTC	2	350	Lung	1.5	Negative	US/CT imaging and follow-up	65.7	17.5	+
						LN, cervical	0.6	Positive	Rx-WBS			
18	Male	59	FTC	2	300	Lung	1.0	Negative	US/CT imaging and follow-up	10.4	21.9	NA
19	Female	39	PTC	4	570	Lung	1.2	Positive	Rx-WBS	208	16.2	NA
20	Female	50	PTC	3	600	Lung	1.2	Positive	Pathology	289	20.6	NA
						Left pleura	0.6	Positive	Rx-WBS			
21	Female	37	PTC	2	350	LN, parapharyngeal	1.2	Positive	Rx-WBS	4.79	17.8	NA
						Lung	0.4	Positive	Rx-WBS			
22	Female	43	PTC	3	550	Lung	0.5	Negative	US/CT imaging and follow-up	64.6	18.1	+
23	Female	49	PTC	4	750	Lung	1.3	Positive	Pathology	1497	15.3	NA
						Paratracheal nodule	1.0	Positive	Rx-WBS			
24	Female	58	PTC	2	230	LN	0.8	Negative	US/CT imaging and follow-up	879	< 15	NA
						Lung	1.5	Positive	Rx-WBS			

Table 1 (continued)

Patient no.	Gender	Age	Pathologic type	No of RAI	Accumulated dose (mCi)	Metastatic lesions		Last Rx-WBS	Confirmation of metastatic lesions	TG (ng/mL)	TGAb (IU/mL)	$BRAFV^{600E}$ mutation
						Site	Size (cm)					
						Bone, C6	–	Negative	US/CT imaging and follow-up			
						Paratracheal nodule	1.5	Negative	US/CT imaging and follow-up			

RAI radioactive iodine, *Rx-WBS* post-therapeutic radioiodine whole body scan, *TG* thyroglobulin, *TGAb* antithyroglobulin antibody, *PTC* papillary thyroid cancer, *FTC* follicular thyroid cancer, *LN* lymph node, *NA* not available

Response Evaluation Criteria in Solid Tumors (RECIST) 1.1 [18]. The target lesions including lung metastases which were greater than 10 mm by CT scan and malignant LNs which were greater than 15 mm in short axis when assessed by CT scan (CT scan slice thickness recommended to be no greater than 5 mm).

The region of interest (ROI) was drawn manually on the entire target lesions on PET cross-sections. The maximum standardized uptake value (SUVmax) and the average standardized uptake value (SUVmean) was calculated for the quantitative analysis. The target-to-background ratio (TBR) was calculated by dividing the lesion SUVmax by the SUVmean of the ascending aorta. The normal organs were evaluated with a 1-cm-diameter (for the small organs [parotid gland and submaxillary gland]) to 2-cm-diameter (liver, spleen, bone marrow and kidney) sphere placed inside the organ parenchyma [9].

The size of well-defined metastatic lesions such as lung and LNs was measured. Lung metastases were measured by the longest diameter in the axial plane. The size of the metastatic LN was determined by the short diameter of the CT cross-section. The mean growth rates of target lesions were defined as follows: [(lesion size in FAPI imaging-lesion size 6 months ago)/lesion size 6 months ago] × 100%. The clinical data of the patients were recorded in detail for subsequent analysis. Serum thyroid stimulating hormone (TSH), TG, and antithyroglobulin (TGAb) levels were measured before ^{68}Ga-DOTA-FAPI-04 PET/CT imaging by an electrochemiluminescent immunoassay on a Cobas analyzer (CCM + cobas8000, Roche Ltd., Basel, Switzerland). The correlation between SUVmax and growth rates of the target lesions was analyzed. Meanwhile, the relationship between SUVmax and TG was studied in patients with negative TGAb.

Immunohistochemistry of FAP expression

Immunohistochemical staining of FAP was performed on the tumor tissue obtained from biopsy specimens in one patient with pleural metastasis. An antibody against FAP (ab207178, Abcam) was used.

Statistical analysis

Statistical analysis was performed using SPSS Statistics 23 (IBM Inc., Armonk, NY, USA). All quantitative data were expressed as mean ± standard deviation or as medians with ranges. Kruskal–Wallis test was used to compare median values. The correlation between the two variables was performed by Spearman correlation analysis. A p value of less than 0.05 was set as indicating a statistical significance.

Results

Patients' characteristics

We analyzed the data for 24 RR-DTC patients (7 men and 17 women; 49.6 ± 10.5 year; 25–66 years) in our center from December 2020 to November 2021. Majority patients (22/24) had papillary thyroid cancer (PTC) histotype. Among these patients, the metastatic tissues of 10 patients did not ever concentrate ^{131}I, ^{131}I is concentrated in some lesions of 3 patients but not in others, the tumor tissue loses the ability to concentrate ^{131}I after previous evidence of ^{131}I-avid disease (in the absence of stable iodine contamination) in 3 patients, and metastatic disease in other 8 patients progressed despite significant concentration of ^{131}I. The enrolled patients received an average of 3.87 times of ^{131}I treatment, and the average activity was 24.24 GBq. Patient 2# has been taking donafenib tosilate tablets 0.3 g bid for 28 months, patients 8# and 19# have been taking apatinib mesylate tablets for over 28 months and 34 months, respectively. Patient 1# had been treated with donafenib tosilate tablets 0.3 g bid 1 week and stopped because of a severe allergic reaction. The rest subjects only received levothyroxine therapy after the last ^{131}I treatment. TSH level of all patients enrolled was less than 0.01 mIU/L. Except of 1 patient who had high TGAb (2854 IU/mL), the mean TG level of the rest patients was 791.7 ng/mL. BRAF^{V600E} mutations were detected in 4/24 patients. Three patients had positive BRAF^{V600E} mutation, while only one patient had negative (Table 1).

According to pathological results, clinical information and follow-up, 6 patients had bone metastasis, including patient 14# with only bone metastasis. Majority of enrolled patients (23/24) had lung metastasis. There were 3 cases of pleural metastasis. Metastases involving both LN and distant organs were revealed in 12 patients. The detailed clinical characteristics of the enrolled patients are summarized in Table 1.

Detection of patient-based RR-DTC metastasis

Positive metastases were detected in 87.5% (21/24) patients. Majority of the patients (23/24) were complicated with lung metastasis, among which 6 patients had negative FAPI imaging of lung metastasis. Twelve patients had LN metastasis, of which 3 patients had no abnormal FAPI uptake of lymph node metastasis. The typical positive image of ^{68}Ga-DOTA-FAPI-04 PET/CT and detailed illustration of the enrolled patients are presented in Fig. 1 and Table 2.

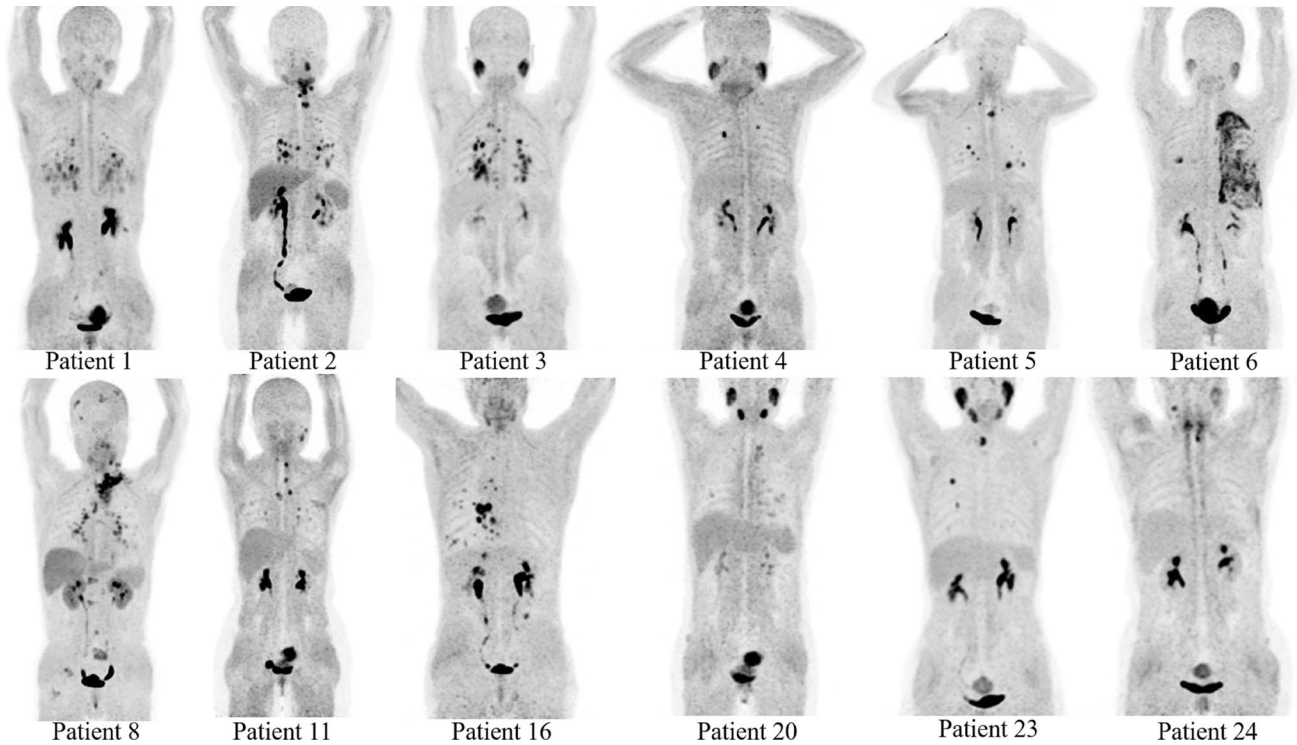

Fig. 1 ^{68}Ga-DOTA-FAPI-04 PET maximum-intensity-projection images of 12 patients with metastatic and recurrent RR-DTC lesions

Table 2 ^{68}Ga-FAPI-04 PET/CT image of 24 RR-DTC patients

Patient no.	Metastatic lesions	SUVmax	TBR	SUVmean				
				Liver	Spleen	Bone marrow	Parotid gland	Submaxillary gland
1	Lung	6.3	8.97	0.87	0.86	0.36	1.87	2.68
2	Thyroid Bed	13.5	17.1	2.57	2.37	0.38	1.04	2.55
	LN	7.2	9.12					
	Lung	10.6	13.43					
	Bone	7.5	9.5					
3	LN	9.6	9.16	1.41	1.41	0.50	6.4	2.4
	Lung	10.4	9.93					
4	Lung	9	9.18	1.34	1.49	0.46	6.32	4.6
5	LN	9.9	8.23	2.17	1.70	0.41	1.47	1.88
	Lung	12	9.98					
6	Lung	4.7	6.9	1.12	1.13	0.92	2.97	1.54
	Pleura	10.3	15.12					
	LN	–	–					
7	Lung	–	–	0.77	0.93	0.34	0.77	1.61
8	LN	10.2	8.85	2.60	2.00	0.68	1.07	2.60
	Lung	3.1	2.69					
	Bone	5.8	5.03					
9	LN	2.4	2.62	1.77	2.05	0.41	2.33	2.46
	Lung	–	–					
10	Lung	5.1	4.4	1.01	1.19	0.49	1.78	2.10
11	LN	6.7	8.93	2.0	1.51	0.45	0.74	1.23
	Lung	3.4	4.53					
12	Lung	5.1	3.4	0.98	1.22	0.48	1.65	2.37
	LN	–	–					
13	Bone	4.1	1.32	2.58	3.17	0.93	1.54	2.18
	Lung	–	–					
14	Bone	6.08	4.05	1.90	1.45	0.45	2.79	2.04
15	Lung	2.1	2.1	1.66	1.65	0.45	3.37	2.94
16	LN	8.2	10.12	1.01	0.68	0.48	1.37	2.51
	Lung	10.2	12.59					
	Bone	4.2	5.18					
	Pleura	5.0	6.17					
17	Lung	8.7	8.96	1.12	0.94	0.46	1.51	2.84
	LN	–	–					
18	Lung	–	–	1.82	1.49	0.34	1.05	1.39
19	Lung	–	–	3.08	2.47	0.54	3.24	2.55
20	Lung	2.25	2.29	2.24	2.19	0.60	6.5	10.07
	Pleura	4.7	4.79					
21	LN	2.28	3.16	2.75	1.50	0.40	7.43	2.37
	Lung	–	–					
22	Lung	1.0	1.4	1.6	1.19	0.42	3.26	2.87
23	Lung	8.2	8.36	1.92	2.07	0.38	8.6	7.4
	Paratracheal nodule	8.4	8.57					
24	LN	6.4	6.66	1.63	1.60	0.52	2.39	2.65
	Lung	1.44	1.5					
	Bone	8.3	8.64					
	Paratracheal nodule	7.99	7.07					

LN lymph node, *TBR* tumor-to-background, *SUVmax* the maximum standardized uptake value, *SUVmean* the average standardized uptake value

Detection of all-lesion-based RR-DTC metastasis

Most of the lesions were positive on ^{68}Ga-DOTA-FAPI-04 PET/CT images, including LN metastasis and distant metastasis such as lung, bone and pleura (Figs. 2, 3). A total of 118 well-defined metastatic lesions were included in the analysis, including 11 LN lesions, 80 lung lesions and 27 bone lesions. Median size of metastatic LN and lung lesions measured 0.9 cm (range 0.8–2.3 cm) and 1.0 cm (range 0.6–2.7 cm), respectively. The mean SUVmax of LN, lung, and bone metastasis was 7.06 ± 0.39, 6.39 ± 0.91 and 4.01 ± 0.48 ($p = 0.000$), respectively. The mean TBR of LN, lung, and bone metastasis was 7.96 ± 1.57, 4.29 ± 3.07 and 3.35 ± 1.90 ($p = 0.000$), respectively. SUVmax was statistically associated with the metastatic organs ($p = 0.000$). While SUVmax was not statistically associated with the serum TG levels before the PET scan ($p = 0.139$).

All bone metastasis were clearly displayed (Fig. 3). A total of 27 bone metastatic lesions were found, including 3 in skulls, 2 in sternum, 2 in clavicles, 1 in rib, 11 in vertebrae, 6 in pelvis and 2 in femurs. Osteolysis, osteogenesis and mixed type of bone metastasis were 14, 4 and 9, respectively. The mean SUVmax of osteolysis, osteogenesis and mixed bone metastasis was 4.16 ± 0.52, 2.14 ± 0.39 and 4.15 ± 0.31, respectively. The mean TBR of osteolysis, osteogenesis and mixed bone metastasis was 3.88 ± 0.64, 1.77 ± 0.32 and 3.24 ± 0.17, respectively.

Detection of target lesion-based RR-DTC metastasis

There were altogether 33 target lesions including 30 lung metastases and 3 LN metastases in 11 patients for the detection of the mean growth rates. In patient 4# and 24#, there was no follow-up CT images in the past 6 months.

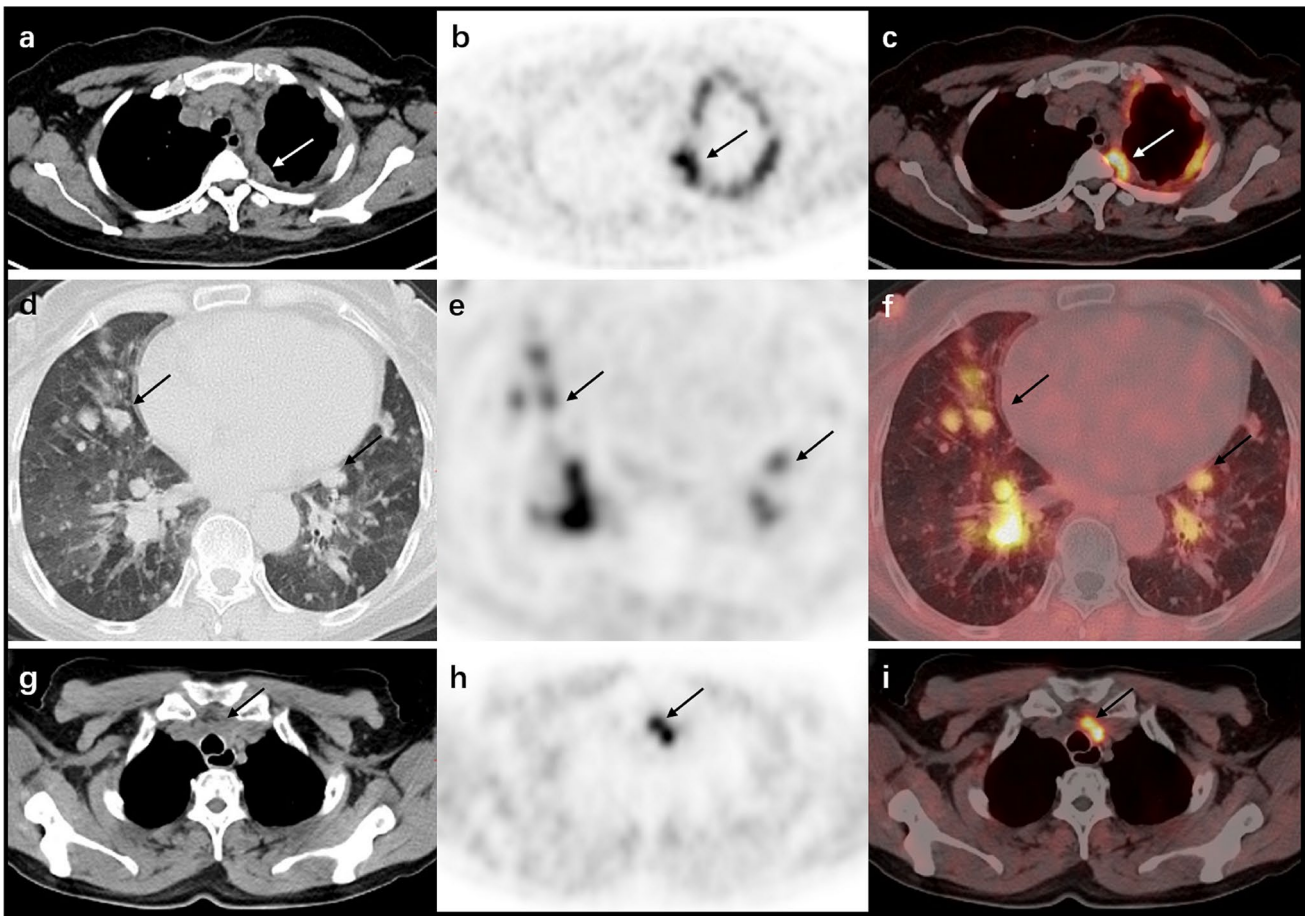

Fig. 2 A 43-year-old female with left pleura metastasis was referred to ^{68}Ga-DOTA-FAPI-04 PET/CT imaging (**a** axial CT; **b** axial ^{68}Ga-DOTA-FAPI-04 PET; **c** axial fusion image) which revealed multiple intense FAPI-avid nodules of the left pleura (as indicated by the arrow). A 62-year-old female with lung metastasis underwent ^{68}Ga-DOTA-FAPI-04 PET/CT imaging (**d** axial CT; **e** axial ^{68}Ga-DOTA-FAPI-04 PET; **f** axial fusion image) which revealed multiple nodules with intermediate to high uptake of FAPI of bilateral lungs (as pointed by the arrow). A 59-year-old female with lymph node metastasis underwent ^{68}Ga-DOTA-FAPI-04 PET/CT imaging (**g** axial CT; **h** axial ^{68}Ga-DOTA-FAPI-04 PET; **i** axial fusion image) which revealed the strong FAPI-avid lymph nodes in the mediastinum (as shown by the arrow)

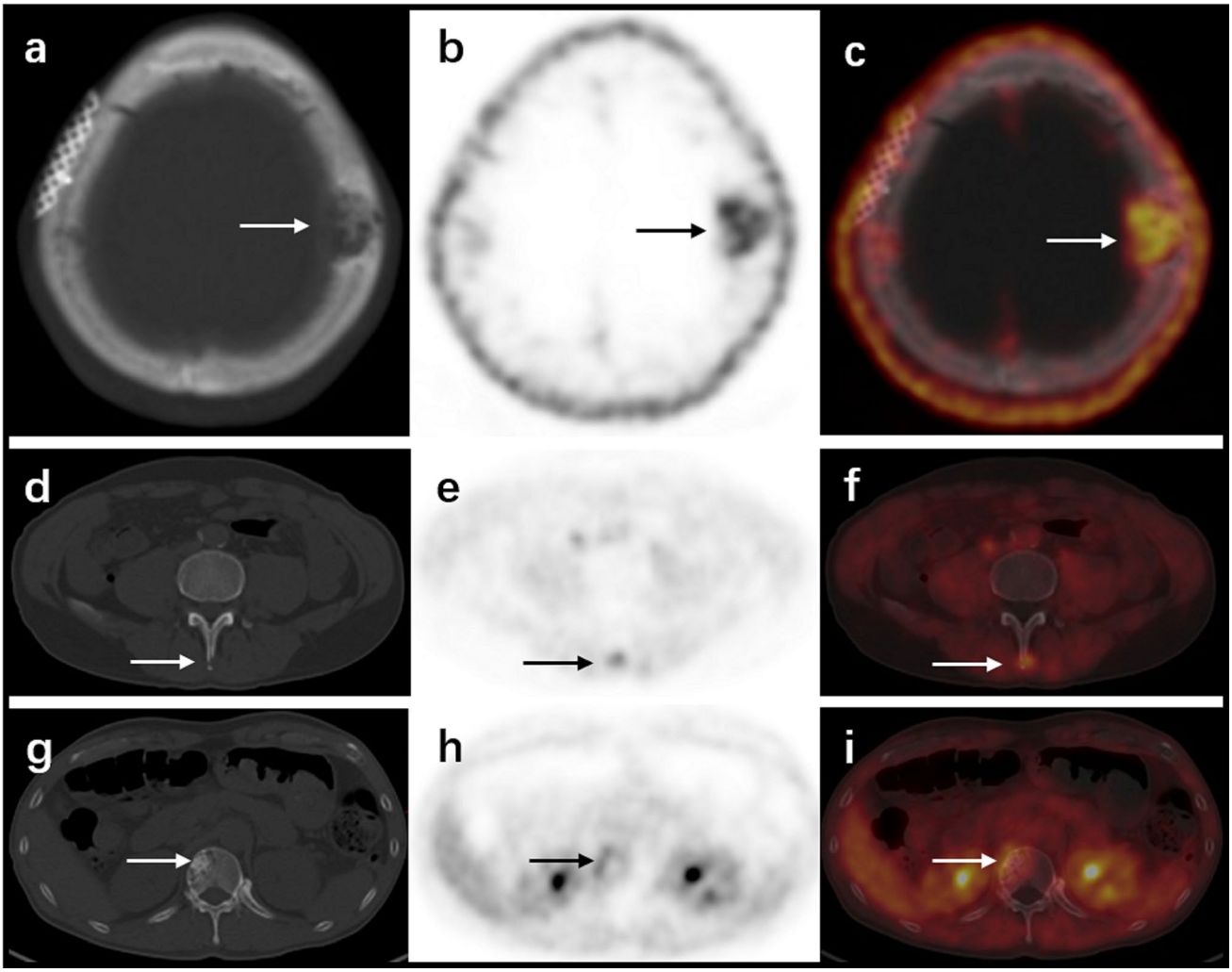

Fig. 3 A 52-year-old male with bone metastasis was referred to ^{68}Ga-DOTA-FAPI-04 PET/CT imaging (**a**, **d**, **g**, axial CT; **b**, **e**, **h**, axial ^{68}Ga-DOTA-FAPI-04 PET; **c**, **f**, **i**, axial fusion image) which revealed the skull and vertebrae lesions with mild-to-moderate uptake of FAPI, including mixed (**a**), osteolytic (**d**), and osteogenic (**g**) metastatic lesions (as pointed by the arrow)

The mean SUVmax and the growth rate of the target lesions was 4.25 and 6.51%, respectively. Spearman's rank correlation test revealed a positive correlation between the growth rates of the target lesions and SUVmax ($r = 0.348$, $p = 0.047$) (Fig. 4).

Detection of non-target lesion-based RR-DTC metastasis

Metastatic lung lesions with a diameter smaller than 1 cm were defined as non-target lesions. All patients with lung metastasis had non-target lesions. SUVmax, fluctuated between 0.7 and 4.4, was hard to match non-target lesions correctly because of the patients' respiratory movement. The total number is difficult to determine and meaningless.

Immunohistochemistry

One pleural metastatic tumor sample obtained from patient 6# was assessed for FAP expression by immunohistochemistry. Stromal cells around the tumor had prominent FAP expression. ^{68}Ga-DOTA-FAPI-04 PET showed high uptake (SUVmax = 10.3) in the pleural metastasis of this patient [19].

Organ distribution of ^{68}Ga-DOTA-FAPI-04 PET/CT imaging in RR-DTC patients

^{68}Ga-DOTA-FAPI-04 PET imaging of 24 patients with metastatic RR-DTC resulted in no adverse events. Except for the accumulation in the kidney and bladder due to the main excretion pathway, most patients (23/24) had

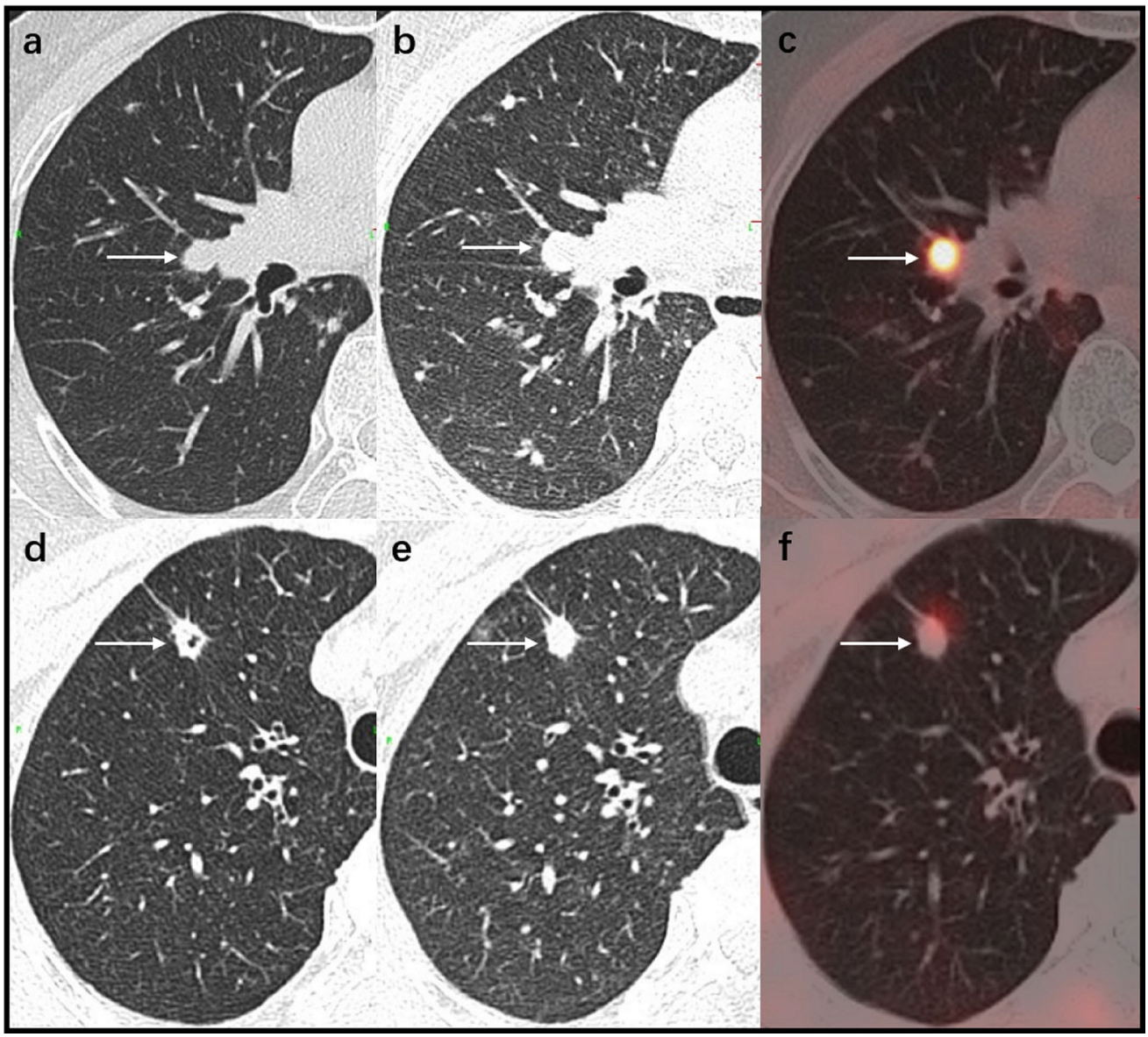

Fig. 4 A 59-year-old female with lung metastasis underwent ^{68}Ga-DOTA-FAPI-04 PET/CT imaging comparing with her chest CT scan 6 months ago. In axial CT image 6 months ago, the metastatic pulmonary nodule (white arrow) measured 13.7 mm (**a** axial CT) and 10 mm (**d** axial CT), respectively. In ^{68}Ga-DOTA-FAPI-04 PET/CT imaging, the target lesions measured 16.1 mm (**b** axial CT) and 11 mm (**e** axial CT) with SUVmax of 12.0 (**c** axial fusion image) and 4.1 (**f** axial fusion image), respectively

only mild ^{68}Ga-DOTA-FAPI-04 uptake in the renal parenchyma. Patient 8# had moderate uptake in renal parenchyma (SUVmean, 2.61) who had proteinuria 2 + (Fig. 1). The mean SUVmean of parotid gland and the submaxillary gland were 2.97 ± 0.47 and 2.90 ± 0.39, respectively. The mean SUVmean of liver, spleen and bone marrow were 1.74 ± 0.13, 1.59 ± 0.11 and 0.49 ± 0.03, respectively.

Discussion

In our study, the results proved moderate-to-high ^{68}Ga-DOTA-FAPI-04 avid in majority metastatic and recurrent RR-DTC lesions. LN and distant metastasis such as lung, pleura, and bone could be clearly detected by ^{68}Ga-DOTA-FAPI-04 PET with statistical difference in

the uptake degree. Osteolytic, osteogenic or mixed bone metastases can be clearly demonstrated. Meanwhile, the lesions with higher SUVmax progress faster in a short term, suggesting that the expressions of FAP are related to the progression of the disease (Fig. 4), which is in line with previous studies [20]. To our knowledge, this study was the first attempt of FAPI-04 PET imaging in 24 RR-DTC patients.

There was no obvious FAPI-04 uptake in metastatic lesions of 3 patients (patient 7#, 18# and 19#). We found that the number of lesions in these patients was less than 10 and the diameter of lesions was less than 1 cm. Two patients with relative low TG level (13.1 ng/ml and 10.4 ng/ml) indicated that the tumor load in these two patients were lower than the others, which may be related to the lower uptake of FAPI. This needs to be confirmed by further research. Except moderate FAPI-avid lung metastases were found in patient 4# with low TG level (3.74 ng/ml), other patients with intense FAPI-avid lesions had high TG levels (range 57.8—> 5000 ng/ml). This finding is consistent with the results of the case previously reported by Fu [21]. There was no statistical significance between SUVmax of metastatic lesions and TG level in this study. The results showed that there was no correlation between the level of TG and the expression of FAP.

The management of RR-DTC metastatic lesions has caused a dilemma. Surgery is not eligible for multiple metastases. ^{131}I cannot be concentrated by RR-DTC metastasis or effectively kill tumor cells [22]. In the last decade, TKIs such as sorafenib and lenvatinib have been approved for the treatment of progressive RR-DTC based on phase III clinical trials [23, 24]. However, TKI is not a specific targeted drug for RR-DTC, because it mainly targets vascular endothelial growth factor receptor (VEGFR) [24], which plays an anti-tumor effect mainly by inhibiting tumor neovascularization. And the relatively high incidence of side effects such as hand-foot syndrome, diarrhea, and hypertension also limit the clinical application of TKIs [25]. Personalized therapy is highly desirable for these patients. In recent years, targeted radionuclide therapy (TRT) in neuroendocrine tumor and prostate cancer have shown good effect [26–28]. But there are no suitable radioactive drugs for TRT in RR-DTC patients. Unlike ^{18}F-FDG, DOTA-FAPI can also be labeled with various therapeutic radionuclides such as ^{90}Y, ^{177}Lu and ^{225}Ac. Tadashi Watabe et al. have successfully proved the concept that α-therapy targeting FAP in the cancer stroma is effective [29]. Ballal S et al. have reported ^{177}Lu-DOTA.SA.FAPi radionuclide therapy in an end-stage breast cancer patient [30]. Therefore, FAP may be a promising target for theranostics. FAPI is not specific for de-differentiated thyroid cancer. However, in this study, intermediate to high uptakes of ^{68}Ga-DOTA-FAPI-04 were observed in RR-DTC lesions, and strong FAP expression in stromal cells was confirmed by immunohistochemistry in such lesions [19]. Based on previous study and our findings, TRT based on FAPI may be presented as an alternative to RR-DTC [21, 29, 30].

In this study, mild-to-moderate ^{68}Ga-DOTA-FAPI-04 uptake was found in the liver, spleen, renal and bone marrow, which were consistent with those of previous studies [6, 9]. We noticed that the intense uptake of ^{68}Ga-DOTA-FAPI-04 in parotid gland and submaxillary gland had been found in 7 patients. This may be owing to the atrophy of the secretory parenchyma and salivary gland fibrosis which caused by several times of ^{131}I treatment [31, 32]. It reminds us to pay attention to parotid gland protection in the future FAP TRT.

There are some limitations in this study. The main limitation of this study is that most of the lesions have not been confirmed by pathology. After all, it is unethical to perform pathological biopsies on all suspected lesions with abnormally high uptake of ^{68}Ga-DOTA-FAPI-04 to validate PET/CT results. The second limitation is that these RR-DTC patients did not undergo ^{18}F-FDG PET/CT examination simultaneously, so it remains unknown the added value of FAPI PET/CT compared to FDG PET, which needs further research.

Conclusion

In this study, intermediate to high uptakes of ^{68}Ga-DOTA-FAPI-04 were observed in RR-DTC lesions. ^{68}Ga-DOTA-FAPI-04 PET/CT is a promising modality for diagnosing and opening up new application for radioligand therapy in RR-DTC.

Funding This study was funded in part by the National Natural Science Foundation of China (NSFC) 81971651, 82171982. Natural Science Foundation of Fujian 2019J01454, 2020J05249. Fujian Provincial Health Commission Science and Technology and Programme 2020GGA045.

Declarations

Conflict of interest The authors declare that they have no conflict of interest.

Ethical approval The study was approved by the institutional review board of our hospital and written informed consent for publication of this report was obtained from the patients.

References

1. Sung H, Ferlay J, Siegel RL, Laversanne M, Soerjomataram I, Jemal A, Bray F. Global cancer statistics 2020: GLOBOCAN

estimates of incidence and mortality worldwide for 36 cancers in 185 countries. CA Cancer J Clin. 2021. https://doi.org/10.3322/caac.21660.
2. Durante C, Haddy N, Baudin E, Leboulleux S, Hartl D, Travagli JP, Caillou B, Ricard M, Lumbroso JD, De Vathaire F, Schlumberger M. Long-term outcome of 444 patients with distant metastases from papillary and follicular thyroid carcinoma: benefits and limits of radioiodine therapy. J Clin Endocrinol Metab. 2006;91(8):2892–9.
3. Haugen BR, Alexander EK, Bible KC, Doherty GM, Mandel SJ, Nikiforov YE, Pacini F, Randolph GW, Sawka AM, Schlumberger M, Schuff KG, Sherman SI, Sosa JA, Steward DL, Tuttle RM, Wartofsky L. 2015 American thyroid association management guidelines for adult patients with thyroid nodules and differentiated thyroid cancer: the american thyroid association guidelines task force on thyroid nodules and differentiated thyroid cancer. Thyroid. 2016;26(1):1–133.
4. Garin-Chesa P, Old LJ, Rettig WJ. Cell surface glycoprotein of reactive stromal fibroblasts as a potential antibody target in human epithelial cancers. Proc Natl Acad Sci USA. 1990;87(18):7235–9.
5. Hamson EJ, Keane FM, Tholen S, Schilling O, Gorrell MD. Understanding fibroblast activation protein (FAP): substrates, activities, expression and targeting for cancer therapy. Proteomics Clin Appl. 2014;8(5–6):454–63.
6. Lindner T, Loktev A, Altmann A, Giesel F, Kratochwil C, Debus J, Jäger D, Mier W, Haberkorn U. Development of quinoline-based theranostic ligands for the targeting of fibroblast activation protein. J Nucl Med. 2018;59(9):1415–22.
7. Chen H, Pang Y, Wu J, Zhao L, Hao B, Wu J, Wei J, Wu S, Zhao L, Luo Z, Lin X, Xie C, Sun L, Lin Q, Wu H. Comparison of [(68)Ga]Ga-DOTA-FAPI-04 and [(18)F] FDG PET/CT for the diagnosis of primary and metastatic lesions in patients with various types of cancer. Eur J Nucl Med Mol Imaging. 2020;47(8):1820–32.
8. Chen H, Zhao L, Ruan D, Pang Y, Hao B, Dai Y, Wu X, Guo W, Fan C, Wu J, Huang W, Lin Q, Sun L, Wu H. Usefulness of [(68)Ga]Ga-DOTA-FAPI-04 PET/CT in patients presenting with inconclusive [(18)F]FDG PET/CT findings. Eur J Nucl Med Mol Imaging. 2021;48(1):73–86.
9. Giesel FL, Kratochwil C, Lindner T, Marschalek MM, Loktev A, Lehnert W, Debus J, Jäger D, Flechsig P, Altmann A, Mier W, Haberkorn U. (68)Ga-FAPI PET/CT: biodistribution and preliminary dosimetry estimate of 2 DOTA-containing FAP-targeting agents in patients with various cancers. J Nucl Med. 2019;60(3):386–92.
10. Kratochwil C, Flechsig P, Lindner T, Abderrahim L, Altmann A, Mier W, Adeberg S, Rathke H, Röhrich M, Winter H, Plinkert PK, Marme F, Lang M, Kauczor HU, Jäger D, Debus J, Haberkorn U, Giesel FL. (68)Ga-FAPI PET/CT: tracer uptake in 28 different kinds of cancer. J Nucl Med. 2019;60(6):801–5.
11. Koerber SA, Staudinger F, Kratochwil C, Adeberg S, Haefner MF, Ungerechts G, Rathke H, Winter E, Lindner T, Syed M, Bhatti IA, Herfarth K, Choyke PL, Jaeger D, Haberkorn U, Debus J, Giesel FL. The role of (68)Ga-FAPI PET/CT for patients with malignancies of the lower gastrointestinal tract: first clinical experience. J Nucl Med. 2020;61(9):1331–6.
12. Röhrich M, Loktev A, Wefers AK, Altmann A, Paech D, Adeberg S, Windisch P, Hielscher T, Flechsig P, Floca R, Leitz D, Schuster JP, Huber PE, Debus J, von Deimling A, Lindner T, Haberkorn U. IDH-wildtype glioblastomas and grade III/IV IDH-mutant gliomas show elevated tracer uptake in fibroblast activation protein-specific PET/CT. Eur J Nucl Med Mol Imaging. 2019;46(12):2569–80.
13. Shi X, Xing H, Yang X, Li F, Yao S, Zhang H, Zhao H, Hacker M, Huo L, Li X. Fibroblast imaging of hepatic carcinoma with (68)Ga-FAPI-04 PET/CT: a pilot study in patients with suspected hepatic nodules. Eur J Nucl Med Mol Imaging. 2021;48(1):196–203.
14. Rettig WJ, Garin-Chesa P, Healey JH, Su SL, Ozer HL, Schwab M, Albino AP, Old LJ. Regulation and heteromeric structure of the fibroblast activation protein in normal and transformed cells of mesenchymal and neuroectodermal origin. Cancer Res. 1993;53(14):3327–35.
15. Liu B, Zhang Z, Wang H, Yao S. Preclinical evaluation of a dual sstr2 and integrin α(v)β(3)-targeted heterodimer [(68)Ga]-NOTA-3PEG(4)-TATE-RGD. Bioorg Med Chem. 2019;27(21): 115094.
16. Leboulleux S, Girard E, Rose M, Travagli JP, Sabbah N, Caillou B, Hartl DM, Lassau N, Baudin E, Schlumberger M. Ultrasound criteria of malignancy for cervical lymph nodes in patients followed up for differentiated thyroid cancer. J Clin Endocrinol Metab. 2007;92(9):3590–4.
17. Leenhardt L, Erdogan MF, Hegedus L, Mandel SJ, Paschke R, Rago T, Russ G. 2013 European thyroid association guidelines for cervical ultrasound scan and ultrasound-guided techniques in the postoperative management of patients with thyroid cancer. Eur Thyroid J. 2013;2(3):147–59.
18. Eisenhauer EA, Therasse P, Bogaerts J, Schwartz LH, Sargent D, Ford R, Dancey J, Arbuck S, Gwyther S, Mooney M, Rubinstein L, Shankar L, Dodd L, Kaplan R, Lacombe D, Verweij J. New response evaluation criteria in solid tumours: revised RECIST guideline (version 1.1). Eur J Cancer. 2009;45(2):228–47.
19. Chen Y, Zheng S, Zhang J, Yao S, Miao W. Pleural metastasis of papillary thyroid cancer depicted by ^{68}Ga-FAPI PET/CT. Clin Nucl Med. 2022. https://doi.org/10.1097/RLU.0000000000004038.
20. Liu F, Qi L, Liu B, Liu J, Zhang H, Che D, Cao J, Shen J, Geng J, Bi Y, Ye L, Pan B, Yu Y. Fibroblast activation protein overexpression and clinical implications in solid tumors: a meta-analysis. PLoS One. 2015;10(3): e0116683.
21. Fu H, Fu J, Huang J, Su X, Chen H. 68Ga-FAPI PET/CT in thyroid cancer with thyroglobulin elevation and negative iodine scintigraphy. Clin Nucl Med. 2021;46(5):427–30.
22. Van Nostrand D. Radioiodine refractory differentiated thyroid cancer: time to update the classifications. Thyroid. 2018;28(9):1083–93.
23. Schlumberger M, Tahara M, Wirth LJ, Robinson B, Brose MS, Elisei R, Habra MA, Newbold K, Shah MH, Hoff AO, Gianoukakis AG, Kiyota N, Taylor MH, Kim SB, Krzyzanowska MK, Dutcus CE, de las Heras B, Zhu J, Sherman SI. Lenvatinib versus placebo in radioiodine-refractory thyroid cancer. N Engl J Med. 2015;372(7):621–30.
24. Brose MS, Nutting CM, Jarzab B, Elisei R, Siena S, Bastholt L, de la Fouchardiere C, Pacini F, Paschke R, Shong YK, Sherman SI, Smit JW, Chung J, Kappeler C, Peña C, Molnár I, Schlumberger MJ. Sorafenib in radioactive iodine-refractory, locally advanced or metastatic differentiated thyroid cancer: a randomised, double-blind, phase 3 trial. Lancet. 2014;384(9940):319–28.
25. Cheng L, Fu H, Jin Y, Sa R, Chen L. Clinicopathological features predict outcomes in patients with radioiodine-refractory differentiated thyroid cancer treated with sorafenib: a real-world study. Oncologist. 2020;25(4):e668–78.
26. Sorbye H, Kong G, Grozinsky-Glasberg S. PRRT in high-grade gastroenteropancreatic neuroendocrine neoplasms (WHO G3). Endocr Relat Cancer. 2020;27(3):R67-r77.
27. Violet J, Sandhu S, Iravani A, Ferdinandus J, Thang SP, Kong G, Kumar AR, Akhurst T, Pattison DA, Beaulieu A, Mooi J, Tran B, Guo C, Kalff V, Murphy DG, Jackson P, Eu P, Scalzo M, Williams S, Hicks RJ, Hofman MS. Long-term follow-up and outcomes of retreatment in an expanded 50-patient single-center phase II prospective trial of (177)Lu-PSMA-617 theranostics in metastatic castration-resistant prostate cancer. J Nucl Med. 2020;61(6):857–65.

28. Brabander T, van der Zwan WA, Teunissen JJM, Kam BLR, Feelders RA, de Herder WW, van Eijck CHJ, Franssen GJH, Krenning EP, Kwekkeboom DJ. Long-term efficacy, survival, and safety of [(177)Lu-DOTA(0), Tyr(3)]octreotate in patients with gastroenteropancreatic and bronchial neuroendocrine tumors. Clin Cancer Res. 2017;23(16):4617–24.
29. Watabe T, Liu Y, Kaneda-Nakashima K, Shirakami Y, Lindner T, Ooe K, Toyoshima A, Nagata K, Shimosegawa E, Haberkorn U, Kratochwil C, Shinohara A, Giesel F, Hatazawa J. theranostics targeting fibroblast activation protein in the tumor stroma: (64) Cu- and (225)Ac-labeled FAPI-04 in pancreatic cancer xenograft mouse models. J Nucl Med. 2020;61(4):563–9.
30. Ballal S, Yadav MP, Kramer V, Moon ES, Roesch F, Tripathi M, Mallick S, ArunRaj ST, Bal C. A theranostic approach of [(68) Ga]Ga-DOTA.SA.FAPi PET/CT-guided [(177)Lu]Lu-DOTA. SA.FAPi radionuclide therapy in an end-stage breast cancer patient: new frontier in targeted radionuclide therapy. Eur J Nucl Med Mol Imaging. 2021;48(3):942–4.
31. Ahn BC. Reduction of salivary gland damage during radioiodine therapy for differentiated thyroid cancers. Nucl Med Mol Imaging. 2020;54(3):126–7.
32. Klein Hesselink EN, Brouwers AH, de Jong JR, van der Horst-Schrivers AN, Coppes RP, Lefrandt JD, Jager PL, Vissink A, Links TP. Effects of radioiodine treatment on salivary gland function in patients with differentiated thyroid carcinoma: a prospective study. J Nucl Med. 2016;57(11):1685–91.